

# A Model for Interphase Precipitation in V-Microalloyed Structural Steels

RUNE LAGNEBORG and STANISLAW ZAJAC

A model for interphase precipitation, with a predictive capacity, is presented. This article deals with its application to V-microalloyed steels. The model rests on an analysis of the growth of the V-depleted zone ahead of a sheet of V(C,N) particles and the simultaneous advance of the  $\gamma/\alpha$  interface in which it was nucleated. It is shown that volume diffusion of V cannot explain the observed intersheet spacings and that a faster diffusion process is required. It is postulated that the  $\gamma/\alpha$  boundary will bow out some time after a sheet of V(C,N) particles has formed in it. Part of the V in the  $\gamma$  will then be fed to V(C,N) particles in the sheet by boundary diffusion as the  $\gamma$  transforms to  $\alpha$ . The V content at the front will, thus, be lower than the initial content in the austenite. However, the reduction will be less the further the interface has moved away from the sheet of V(C,N) particles. At a sufficient distance, the V content is again high enough to allow new V(C,N) particles to nucleate, and a new sheet of particles will form. Between the two sheets, there will be a ledge (or superledge) that will advance along the first sheet. The height of the ledge will, thus, be determined by the distance in which V(C,N) particles can again be nucleated. The model exhibits reasonably good agreement with observed values of intersheet spacing, with its temperature dependence and transition from interphase to general precipitation, and with its dependence on C, V, and N content. It also provides physically sound explanations of these dependencies.

## I. BACKGROUND

THE precipitation of V carbonitrides in V-microalloyed steels can occur either randomly in ferrite in the wake of the migrating austenite-ferrite ( $\gamma/\alpha$ ) interface (general precipitation) or by interphase precipitation characterized by the development of sheets of particles parallel to the  $\gamma/\alpha$  interface formed repeatedly, with rather regular spacing. Many investigations have shown that, for compositions typical of V-alloyed structural steels, the general precipitation takes place at lower temperatures, typically below 700 °C, and the interphase precipitation takes place at higher temperatures.

Figure 1 shows the typical morphology of interphase precipitation of V(C,N) in microalloyed 0.10 pct C-0.12 pct V steels. Already, from its appearance, one can conclude that such a microstructure is formed by repeated nucleation of particles in the  $\gamma/\alpha$  interface as the transformation front moves through the austenite. For this type of steel composition, it is normally observed in the temperature range from 800 °C to 700 °C. Despite its clear relation to the migrating  $\gamma/\alpha$  interface, there has been discussion in the literature regarding whether the interphase precipitation nucleates in the boundary, ahead of it in the austenite, or behind it in the ferrite. However, firm experimental evidence now exists that shows that it actually nucleates in the interface.<sup>[1]</sup> By electron microscopy of steels with high alloy contents that stabilize the austenite to room temperature, it has been possible to directly observe V(C,N) particles in the  $\gamma/\alpha$  boundary. Also, from a very general viewpoint, it is to be expected that, in

some high-temperature region where the chemical driving force for precipitation is low, nature chooses the sites where nucleation is energetically most favored, *viz.*, the interface. At lower temperatures where the driving force is large, we might expect general nucleation in the ferrite matrix to occur.

At high transformation temperatures,  $\sim 800$  °C, for typical compositions of V-microalloyed structural steels, the interphase precipitation consists of irregularly spaced and often curved sheets of V(C,N) particles. With decreasing temperatures, the occurrence of curved rows of precipitates diminishes and the dominant mode is regularly spaced, planar sheets of particles (Figure 1). Below about 700 °C, the interphase precipitation is commonly found to be less frequent, and random precipitation from supersaturated ferrite after the  $\gamma/\alpha$  transformation takes over progressively with decreasing temperature.

A characteristic feature of interphase precipitation is that it becomes more refined at lower temperatures, as confirmed by many investigations.<sup>[2,3]</sup> This is demonstrated for the intersheet spacing in 0.10 pct C-0.12 pct V steels in Figure 2. The interparticle spacing within the sheets of precipitation and the precipitate size also decrease with temperature, as might be expected. We may also notice that the particle spacing is notably shorter within a sheet than between sheets. Figures 1 and 2 show that the intersheet spacing is affected considerably by the nitrogen content of the steel. As is evident, it is diminished to almost one-third at 750 °C on increasing the nitrogen content from 0.005 to 0.026 pct.

V(C,N), which has an fcc structure, forms in ferrite as semicoherent discs with an orientation relationship to ferrite of  $(001)_\alpha // (001)_{V(C,N)}$ ,  $(110)_\alpha // (100)_{V(C,N)}$ , first established by Baker and Nutting (B-N).<sup>[4]</sup> The discs are parallel to  $(110)_\alpha$ . Many electron microscopy studies have shown that V(C,N) in interphase precipitation exhibits a single variant out of the three possible in the B-N orientation relationship to  $\alpha$ , contrary to the general precipitation in ferrite, where

RUNE LAGNEBORG, Professor and Former Director of the Institute, and STANISLAW ZAJAC, Group Leader, are with the Mechanical Metallurgy Department, Swedish Institute for Metals Research, S-11428 Stockholm, Sweden.

Manuscript submitted March 21, 2000.

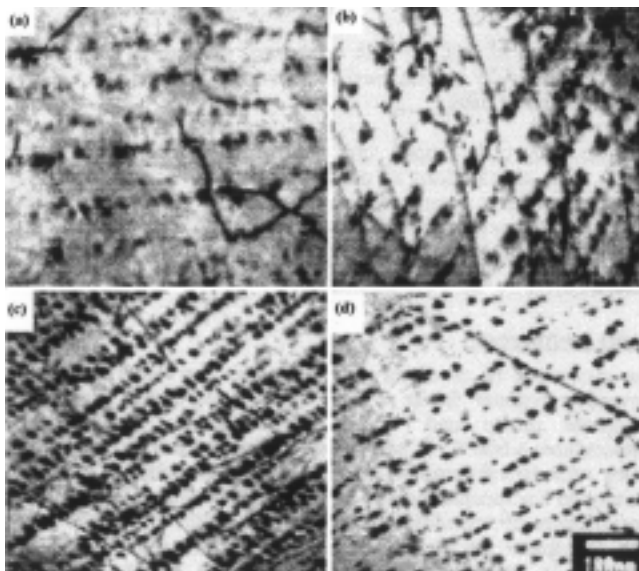


Fig. 1—Electron micrographs illustrating the effect of N in 0.04–0.10 pct C–0.12 pct V steels on the spacing of the precipitate rows and the density of V(C,N) precipitates after isothermal transformation at 750 °C for 500 s: (a) 0.0051 pct N, 0.10 pct C; (b) 0.0082 pct N, 0.10 pct C; (c) 0.0257 pct N, 0.10 pct C; and (d) 0.0095 pct N, 0.04 pct C.<sup>[2]</sup>

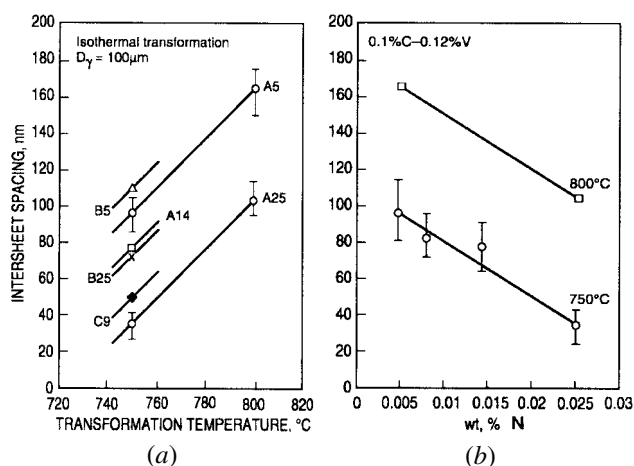


Fig. 2—The effect of (a) transformation temperature and (b) N content on intersheet spacing of V(C,N) interphase precipitation: B5—0.10C–0.06V–0.0056N, A5—0.10C–0.12V–0.0051N, A14—0.10C–0.12V–0.014N, B25—0.10C–0.06V–0.025N, C9—0.04C–0.12V–0.0095N, and A25—0.10C–0.12V–0.026N.<sup>[2]</sup>

all three variants are found.<sup>[5]</sup> This crystallographic selection is given two alternative explanations.<sup>[6,7,8]</sup> In cases where the ferrite and the austenite between which it forms are themselves related by the Kurdjumov–Sachs relationship  $((111)_\gamma // (110)_\alpha)$ , the variant will be chosen that makes the close-packed planes of all three phases parallel. This choice will minimize the free energy for nucleation. In cases without a specific crystallographic  $\gamma/\alpha$  relationship, as for incoherent interfaces, it is suggested that the variant is chosen that puts the disc plane as close as possible to the  $\gamma/\alpha$  boundary, thereby again minimizing the free energy. From this, we realize that the selection of one variant of the B–N orientation relationship is another confirmation of the nucleation of the interphase particles in the  $\gamma/\alpha$  boundary. The observed

selectivity is not compatible with nucleation inside the austenite or the ferrite.

An essential characteristic of the V(C,N) precipitation in these types of steels is the considerable variation of the different modes of precipitation within the same sample and, indeed, within the same grain. This has been observed in many investigations, but has been emphasized in particular by Smith and Dunne.<sup>[5]</sup> Not only is there a variation of the different modes of interphase precipitation, but, as these authors have found, general precipitation occurs both at low and high temperatures and is commonly formed jointly with interphase precipitation in the same grain. They even found general precipitation, confirmed by the occurrence of all three B–N crystallographic variants of V(C,N), at a transformation temperature as high as 820 °C. The explanation they offered for this apparent anomaly is that the first-formed ferrite may grow too rapidly for interphase precipitation to occur, subsequently leaving the ferrite supersaturated for general precipitation.<sup>[5]</sup>

The mechanism of interphase precipitation has been the subject of considerable discussion. The models that have been proposed to explain the phenomenon fall broadly into two categories: ledge mechanisms and models based on solute diffusion control. Honeycombe and co-workers were among the first to study interphase precipitation more profoundly.<sup>[9,10]</sup> They suggested that interphase particles form heterogeneously on  $\gamma/\alpha$  boundaries, thereby pinning their migration normal to the boundary. Local breakaway leads to the formation of mobile ledges. The ledges move sideways while the remaining part of the released boundary is stationary and enables repeated particle nucleation to occur, forming a new sheet. Hence, in this mechanism, the intersheet spacing will be determined by the ledge height. Originally, it was suggested that the  $\gamma/\alpha$  interfaces in which the interphase precipitation formed were semicoherent, immobile  $\{111\}_\gamma / \{110\}_\alpha$  facets. However, later, Ricks and Howell developed the ledge concept further to explain the formation of interphase precipitation in incoherent, often curved  $\gamma/\alpha$  boundaries, usually called the quasi-ledge mechanism.<sup>[11]</sup>

One of the main drawbacks of the ledge mechanism is its inability to produce a credible explanation of the observed variation of the intersheet spacing with temperature and steel composition, especially N, V, and C. It is hard to see how these parameters should generate a variation of the ledge height corresponding to the observed spacings.

Among the models based on diffusion control, the solute-depletion model proposed by Roberts<sup>[12]</sup> is the most prominent and promising one, as it appears to the present authors. In the present model, some of the basic concepts of both this approach and the ledge mechanism have been adopted.

## II. BASIC CONCEPTS OF THE PROPOSED MECHANISM OF INTERPHASE PRECIPITATION

Although experimental investigations<sup>[13]</sup> prior to our own<sup>[2]</sup> have shown a consistent dependence of the intersheet spacing with parameters such as temperature and V content, no previous theory has shown a truly predictive capability of such dependencies. The aim of the present work is to present a physically-chemically sound theory consistent with present knowledge of microalloy-carbonitride precipitation and the  $\gamma/\alpha$  transformation in steels and with a capacity for

reasonable predictions of the dependence of the intersheet spacing on temperature; C, N, and V content; and the transition from interphase to general precipitation.

It is evident from the previous discussion that interphase precipitation results from repetitive nucleation of V carbonitrides in the  $\gamma/\alpha$  interface at distinct intervals as it moves. We consider this as a consequence of the interplay between the growth of the V-denuded zone in front of the sheet of carbonitrides and the simultaneous motion of the  $\gamma/\alpha$  boundary away from the precipitate sheet. These two processes are independent of each other, from the formation of one precipitate row through the motion of the  $\gamma/\alpha$  interface to the point of nucleation of a new row. The following thermodynamic conditions are adopted for the processes.

- (1) Ferrite growth is controlled by C diffusion in austenite, driven by the C gradient ahead of the  $\gamma/\alpha$  interface while maintaining local equilibrium in the interface pseudo-paraequilibrium, according to Hillert.<sup>[14]</sup> This situation will create a thin pileup or trough of alloy elements (depending on whether it is  $\gamma$  or  $\alpha$  that is forming) in austenite just ahead of the moving interface, with a width of  $\sim D_{\text{alloy}}^{\gamma}/\nu$ , where  $\nu$  is the interface velocity. This approach for the  $\gamma/\alpha$  transformation and its validity have been demonstrated in many investigations, *e.g.*, References 15 through 17. It is readily shown that such local equilibrium is valid down to about 700 °C. At lower temperatures, the alloy concentration will be so thin that paraequilibrium prevails in the interface. However, the present model functions in both cases.
- (2) V(C, N) precipitation is controlled by V diffusion, with local equilibrium in the  $\alpha/V(\text{C,N})$  interface and the isoactivity of C and N in ferrite determined by their initial contents in ferrite. Because of the much larger diffusivity of these interstitials in ferrite than in austenite ( $\sim 100$  times greater), this situation is consistent with a C gradient in austenite driving the  $\gamma/\alpha$  transformation. As the V(C,N) precipitation continues, C and N will be consumed and the C and N activity will be gradually lowered. However, in the present work, all computations have been made for the initial contents of C and N dissolved in ferrite.

The drainage of V in the region between the precipitate sheet and the advancing  $\gamma/\alpha$  interface feeds the growth of the V carbonitrides and will initially be rapid when V is available at short distances, but will gradually slow down as V has to be moved over longer distances. The growth rate of ferrite can be considered constant over the short distance of an intersheet spacing. A consequence of the declining rate of V drainage and the constant advance of the ferrite is that the drainage of the V content in the  $\gamma/\alpha$  boundary decreases gradually. At a critical point, the boundary has returned into material with a sufficiently high V content for new nucleation to occur, and a new sheet of precipitates is now formed. These variations in the V content of ferrite in the region between the interphase precipitation and the advancing  $\gamma/\alpha$  interface and in the austenite ahead of the interface are schematically shown in Figure 3. Diffusion of V in austenite is considerably slower than in ferrite, and, accordingly, V drainage in austenite will be very limited, as indicated in the figure.

Any mechanism for interphase precipitation based on nucleation of particles in the interface must be able to

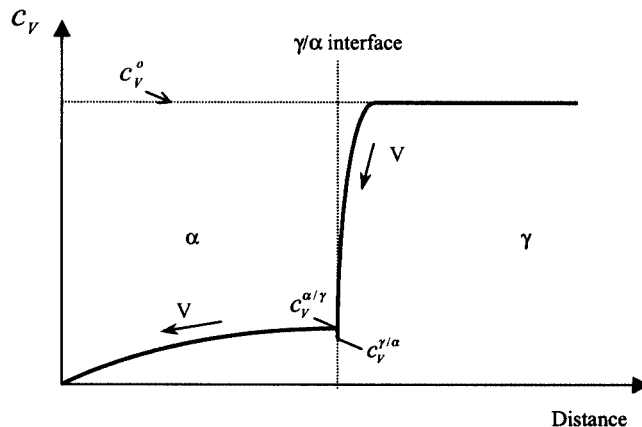


Fig. 3—Schematic figure showing the V profile ahead of and behind an advancing  $\gamma/\alpha$  interface by volume diffusion back to the most recent precipitate row.

account for the release of the boundary from the dense particle population in the precipitate sheet. For the chemical driving force of the  $\gamma/\alpha$  reaction at 750 °C, estimates indicate that particle spacings below about 50 nm will permanently pin the boundary.<sup>[18]</sup> As we can see from the electron micrographs in Figure 1, the spacings are in that range. However, they also show that the spacings vary a great deal and that there are gaps that allow the boundary to bulge locally and then advance.

### III. CONDITION FOR NUCLEATION OF INTERPHASE PRECIPITATION

A necessary part of the present model is a condition for nucleation of V(C,N) in the  $\gamma/\alpha$  interface that can be integrated into the model. We have chosen to handle this problem by first evaluating the minimum V content required for such nucleation ( $C_V^{\alpha/\gamma^*}$ ), using a detailed analysis of electron microscopy observations of interphase precipitation in steels with varying V contents but a given base composition. We have an abundance of such observations for aging at 750 °C at a number of V levels. Based upon those, we judge that interphase precipitation does not occur below 0.034 wt pct at 750 °C in 0.10 pct C-0.010 pct N steels. This will correspond to a critical driving force required for nucleation of V(C,N):  $\Delta G_m$ . By means of the special microalloy database within Thermo-Calc,<sup>[19,20]</sup>  $\Delta G_m$  can be computed for varying solute contents of V, C, and N of the phase from which precipitation occurs and for varying temperatures. For nucleation in a  $\gamma/\alpha$  boundary, the question arises as to whether nucleation should be considered to occur in  $\alpha$  or  $\gamma$  or a mixture of the two. In the present case, local equilibrium, or quasi-paraequilibrium, prevails in the moving interface (*cf.*, Section II). The consequence of this is that the chemical driving force for precipitation of V(C,N) is the same both in the ferrite and in the austenite close to the interface. Since the model to be presented deals with assessment of the V concentration profile in the ferrite up to the point of nucleation in the  $\gamma/\alpha$  interface, we have chosen to present  $\Delta G_m$  and  $C_V^{\alpha/\gamma^*}$  for ferrite. At temperatures below  $\sim 700$  °C, when local equilibrium can no longer be maintained and paraequilibrium prevails, the V content will be uniform across the interface and the concentration in  $\gamma$  close to the interface

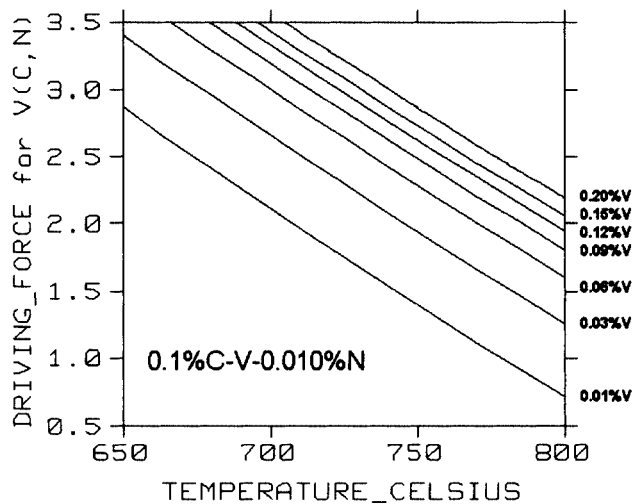


Fig. 4—Chemical driving force for nucleation of V(C,N) in ferrite,  $\Delta G_m/RT$ , as a function of temperature for V-microalloyed steels with 0.1 pct C and 0.01 pct N.

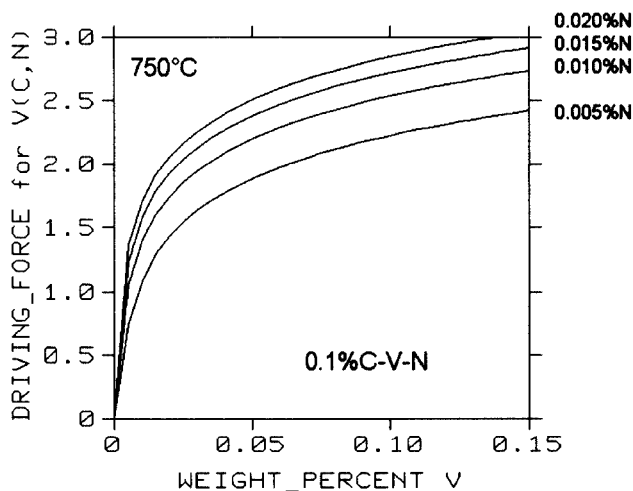


Fig. 5—Chemical driving force for nucleation of V(C,N) in ferrite,  $\Delta G_m/RT$ , at 750 °C as a function of vanadium and nitrogen contents at 0.1 wt pct C.

will increase up to the nominal V content of the steel. This is likely to influence  $c_V^{\alpha/\gamma^*}$  when the region of paraequilibrium is entered (*cf.*, the subsequent comments, where model predictions are compared with observations, Section VI).

Some examples of  $\Delta G_m$  and its dependence on temperature and V and N content are shown in Figures 4 and 5. From Figure 4, we can deduce that 0.034 pct V will correspond to  $\Delta G_m/RT = 2$  at 750 °C in a 0.10 pct C–0.010 pct N steel. Figure 5 demonstrates that  $\Delta G_m$  increases strongly with N content. In turn, this implies that the critical driving force of 2  $RT$  for nucleation is reached for progressively lower V contents as nitrogen increases.

In order to obtain critical V contents for nucleation at other temperatures, but consistent with that of 750 °C, we shall assume that the nucleation rate for interphase precipitation at this critical point is constant with temperature and use the classical expression for nucleation to make the conversion.<sup>[21]</sup>

$$J = \frac{N}{a^2} D_V x_V \cdot \exp\left(-\frac{16\pi\sigma^3 \cdot V_m^2}{3kT \Delta G_m^2}\right) \quad [1]$$

Here,  $J$  is the rate of nucleation,  $N$  is the number of atoms per unit volume,  $a$  is the size of the unit cell,  $D_V$  is the diffusivity of V,  $x_V$  is the molar fraction of V,  $\sigma$  is the  $(\gamma,\alpha)/V(C,N)$  surface energy,  $V_m$  is the molar volume of V(C,N),  $\Delta G_m$  is the molar free energy for formation of V(C,N) from  $\alpha$  of a given composition, and  $k$  and  $T$  have their usual meanings. The temperature dependence of the nucleation rate enters through the factor  $(\Delta G_m)^2 T$  in the exponential of Eq. [1], the diffusivity  $D_V$ , and  $x_V$ , which equals the critical V content for nucleation and is the final result of the conversion. Hence, by initially ignoring the temperature dependence of  $x_V$ , we can compute  $\Delta G_m$  at different temperatures, generating a constant nucleation rate, and then read the corresponding  $c_V^{\alpha/\gamma^*}$  values from graphs such as Figures 4 and 5. By using the  $c_V^{\alpha/\gamma^*}$  values so obtained for  $x_V$ , new  $\Delta G_m$  values and critical V contents are deduced and, by continued iteration, final values are produced, where full account is given to the temperature dependence of  $x_V$ . One of the important results of the present work is that the V transport for interphase precipitation occurs by boundary diffusion in the  $\gamma/\alpha$  interface.

Accordingly, the temperature dependence of V boundary diffusion,  $\exp(-155,000/RT)$ , *cf.*, Section VI, has been used in the conversion. For  $\sigma$  and  $V_m$ , the following values have been employed: 0.32 J/m<sup>2</sup> and 5.46 · 10<sup>-6</sup> m<sup>3</sup>, respectively. The value of  $\sigma$  is in the interval suggested for the interface energy of Nb(C,N)/ $\gamma$  and also contains a factor accounting for heterogeneous nucleation.<sup>[22]</sup>

In Table I, we have listed the critical V contents for nucleation, assessed in the manner described previously, at various temperatures and for various N contents.

When deducing the critical V content at various temperatures, we have chosen only to normalize with respect to the nucleation frequency and not with respect to the velocity of the  $\gamma/\alpha$  interphase. The reason for this will become evident in Sections IV and V, where it is demonstrated that the volume diffusion of V cannot account for interphase precipitation. Instead, the necessary transfer of V will probably occur by more-rapid boundary diffusion in a superledge of the  $\gamma/\alpha$  interphase moving laterally along the precipitate sheet. This implies that the main part of the interface is stationary during the ledge travel; therefore, we consider, once the critical V content is attained, that the dwell time is always sufficient for some nucleation to take place. Admittedly, the duration of the interface stop will affect the nucleation density in the sheet considered, but we should not expect it to influence the occurrence of interphase precipitation as such and, thus, not the intersheet spacing.

#### IV. MODEL FOR INTERPHASE PRECIPITATION CONTROLLED BY VOLUME DIFFUSION OF V

In order to model interphase precipitation and predict the dependence of the intersheet spacing on temperature and alloying contents, we need to describe quantitatively the variation of the V content of ferrite in the  $\gamma/\alpha$  interface as it moves away from the precipitate sheet.

Figure 3 illustrates schematically the variation of the V concentration in the ferrite between a precipitate sheet and

**Table 1. The Critical Driving Force,  $\Delta G_m RT$ , for V(C,N) Interphase Precipitation and the Corresponding Critical V Content,  $c_V^{\alpha/\gamma^*}$**

For 0.10C-0.12V-0.010N Steel at Various Temperatures			For 0.10C-0.12V Steels at 750 °C at Various N Contents		
Temperature	$\Delta G_m/RT$	$c_V^{\alpha/\gamma^*}$ , Wt Pct	N, Wt Pct	$\Delta G_m/RT$	$c_V^{\alpha/\gamma^*}$ , Wt Pct
700 °C	2.55	0.0250	0.005	2	0.064
725 °C	2.28	0.0285	0.010	2	0.034
750 °C	2.00	0.034	0.015	2	0.024
775 °C	1.79	0.044	0.020	2	0.019
800 °C	1.61	0.059	—	—	—
825 °C	1.45	0.086	—	—	—

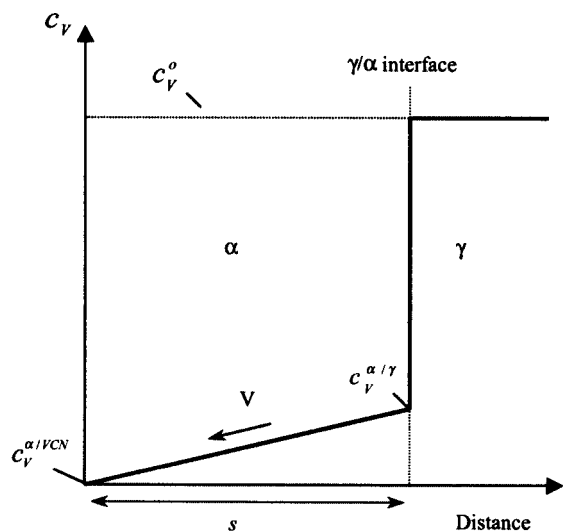


Fig. 6—Simplified variation of the V concentration in the ferrite between a sheet of interphase precipitation and the advancing  $\gamma/\alpha$  interface.

the advancing  $\gamma/\alpha$  interface and in the austenite ahead of the interface, if controlled by volume diffusion toward the sheet of precipitates. Due to the fact that diffusion of V is much greater in ferrite than in austenite, we can neglect the diffusion in austenite. By assuming, furthermore, that the V gradient between the sheet and the interface is linear, the V distribution can be simplified, as shown in Figure 6. As the  $\gamma/\alpha$  interface advances, a V quantity corresponding to the difference between the V content in the austenite and the V content of ferrite in the interface ( $c_V^0 - c_V^{\alpha/\gamma}$ ) is transferred from the austenite into the ferrite and must be moved away through the ferrite by diffusion. The basis of the model is that  $c_V^{\alpha/\gamma}$  is balanced such that the transfer of V across the interface exactly equals the diffusional flow of V through the ferrite. Quantitatively, this mass balance can be expressed as

$$(c_V^0 - c_V^{\alpha/\gamma}) \frac{ds}{dt} = D_V^\alpha \frac{dc_V^\alpha}{ds} = D_V^\alpha \frac{c_V^{\alpha/\gamma} - c_V^{\alpha/VCN}}{s} \quad [2]$$

where  $s$  is the distance between the precipitate sheet and the advancing interface,  $D_V^\alpha$  is the diffusion coefficient of V in  $\alpha$ ,  $c_V^\alpha$  is the V content in  $\alpha$ , and  $c_V^{\alpha/VCN}$  is the V content of  $\alpha$  in the  $\alpha/VCN$  interface. It may be noted that with the simplifications made,  $c_V^{\gamma/\alpha}$  (cf., Figure 3) does not enter the model and, hence, the local equilibrium in the interface needs not to be considered.

Eq. [2] contains the velocity of the  $\gamma/\alpha$  interface ( $ds/dt$ ) and, hence, the model needs a quantitative description of this variable. We will assume that the growth of ferrite into austenite is controlled by C diffusion driven by the C gradient ahead of the  $\gamma/\alpha$  boundary, while maintaining local equilibrium in the interface. By considering the  $\gamma/\alpha$  interface as a planar front growing into austenite and approximating the C pileup in the austenite to have a triangular shape, the following expression describes the ferrite growth.<sup>[23]</sup>

$$S^2 = D_C^\gamma \frac{(c_C^{\gamma/\alpha} - c_C^{\gamma/\infty})^2}{(c_C^{\gamma/\alpha} - c_C^\alpha)(c_C^{\gamma/\infty} - c_C^\alpha)} \cdot t \quad [3]$$

where  $S$  is the distance from the point of  $\alpha$  nucleation to the location of the  $\gamma/\alpha$  interface at time  $t$ ,  $D_C^\gamma$  is the diffusion coefficient of C in austenite,  $c_C^{\gamma/\alpha}$  is the C content of  $\gamma$  at the  $\gamma/\alpha$  interface,  $c_C^{\gamma/\infty}$  is the original C content of  $\gamma$ , and  $c_C^\alpha$  is the C content of  $\alpha$  in equilibrium with  $\gamma$ .

By differentiation of Eq. [3], the velocity of the  $\gamma/\alpha$  boundary is obtained, and  $S$  can be expressed as

$$S = \frac{K_1}{2\nu} = \frac{K_1}{2ds/dt} \quad [4]$$

where  $K_1$  is the proportionality factor in Eq. [3].

The combination of Eqs. [2] and [4] gives the following expression for  $c_V^{\alpha/\gamma} = f(s)$ :

$$\frac{c_V^0 - c_V^{\alpha/\gamma}}{c_V^{\alpha/\gamma} - c_V^{\alpha/VCN}} = \frac{2D_V^\alpha S}{K_1 s} \quad [5]$$

By inserting the critical V contents for nucleation of interphase precipitation ( $c_V^{\alpha/\gamma^*}$ ) into Eq. [5], we arrive at the following relationship for the intersheet spacing:

$$\lambda = \left( \frac{2D_V^\alpha S}{K_1} \right) \frac{c_V^{\alpha/\gamma^*} - c_V^{\alpha/VCN}}{c_V^0 - c_V^{\alpha/\gamma^*}} \quad [6]$$

An essential result of this analysis is that, by adopting data for volume diffusion of V,<sup>[24]</sup> the model predicts intersheet spacings much smaller than those observed. In order to reach agreement between the computed and experimental spacings, the diffusion coefficient for V in  $\alpha$  needs to be increased by a factor of about  $10^4$ . This corresponds to a decrease of the activation energy from 240,000 to 157,000 J/mol, hence, not far from the activation energy we can expect for boundary diffusion. This shows very clearly that the supply of V to the interphase precipitation must occur by a much faster process than volume diffusion. This suggests to us that we must find a mechanism where the V is supplied by fast boundary diffusion in the  $\gamma/\alpha$  interface.

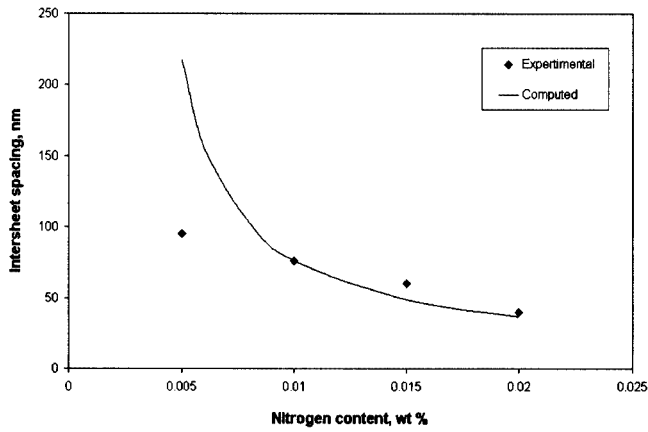


Fig. 7—Comparison between computed and observed intersheet spacings in 0.10C-0.12V steels, aged at 750 °C, as a function of N content.

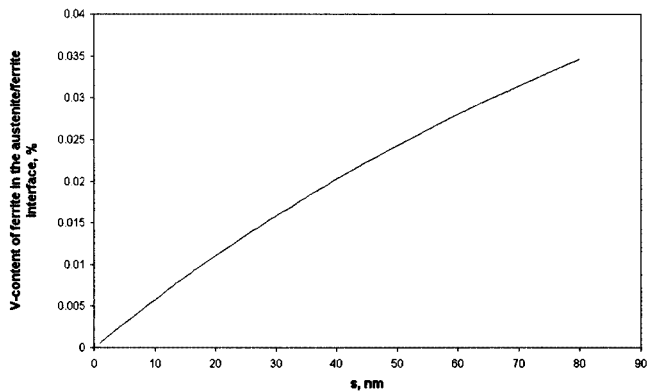


Fig. 8—Variation of  $c_V^{\alpha/\gamma}$  with the advance of the interface according to the volume diffusion model after modifying  $D_V^\alpha$  by a factor of  $10^4$ , 0.10C-0.12V-0.010N steel aged at 750 °C.

Nevertheless, once the diffusion coefficient has been adjusted, the model based on volume diffusion would be capable to predict the dependence of the intersheet spacing with temperature and the C, V, and N contents quite well. An example of this is shown in Figure 7.

Figure 8 shows the computed change of  $c_V^{\alpha/\gamma}$  as the  $\gamma/\alpha$  interface leaves one precipitate sheet and up to the point of nucleation of the next. We may note that  $c_V^{\alpha/\gamma}$  increases almost linearly, and that its rate of increase is only lowered slightly for this range of distances.

## V. MODEL FOR INTERPHASE PRECIPITATION CONTROLLED BY BOUNDARY DIFFUSION OF V IN THE MOVING $\gamma/\alpha$ BOUNDARY

In the following text, we will show that the original explanation of interphase precipitation by Davenport and Honeycombe<sup>[9]</sup> and Honeycombe<sup>[10]</sup> as being a periodic precipitation in semicoherent, immobile  $\{111\}_\gamma/\{110\}_\alpha$  interfaces where the ferrite growth occurs by lateral motion of ledges along the  $\gamma/\alpha$  interface, can be merged with our concept of the interphase precipitation being controlled by the solute drainage behind the moving  $\gamma/\alpha$  boundary. In particular, the ledge mechanism offers a mechanism for the supply of solutes to the growing precipitates behind the advancing  $\gamma/\alpha$

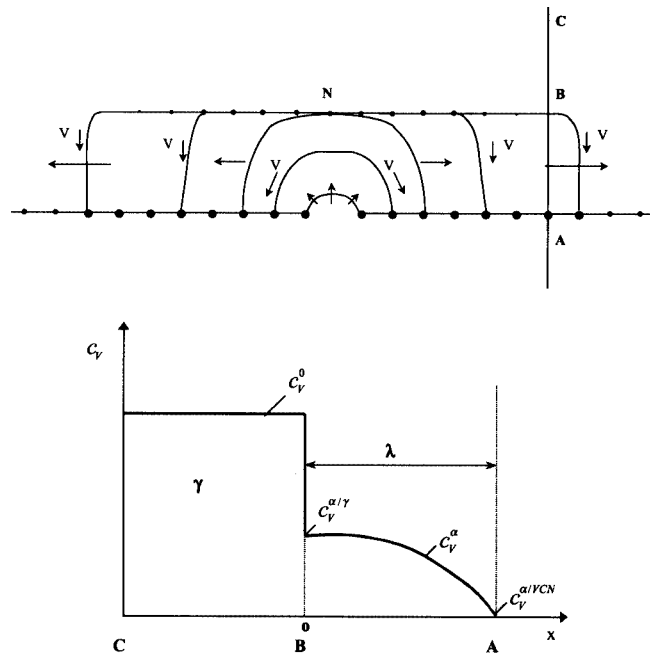


Fig. 9—Top figure shows schematically how the  $\gamma/\alpha$  interface bows out, expands sideways, and eventually reaches material with sufficient V for renewed precipitate nucleation to occur. The transfer of V boundary diffusion to the lower precipitate row is indicated. The lower figure shows the V-content profile in a cross section.

interface by fast boundary diffusion in the moving ledge interface. As we will see, it is also possible to combine the quasi-ledge mechanism proposed by Ricks and Howell<sup>[11]</sup> for interphase precipitation occurring in curved, incoherent non- $\{111\}_\gamma/\{110\}_\alpha$  interfaces with our solute-depletion model. In this way, a complete model can be established that is consistent both with the microscopic observations upon which the models by Honeycombe and Ricks and Howell are founded and with the observed intersheet spacings and their dependence on temperature and alloying contents. The explanation of the latter dependencies has been the particular target of the work by the present authors.

Figure 9 illustrates how we conceive the events in interphase precipitation to occur, from the completion of one precipitate sheet, through the local bulging of the  $\gamma/\alpha$  interface at a point where the precipitates are thinly spaced and its further advance to the position where a new row of particles can be nucleated, and to the lateral spread of the new row of precipitation by motion of two  $\gamma/\alpha$  interface superledges along the lower row of particles.

We will first consider the case of semicoherent, immobile  $\gamma/\alpha$  interfaces. Therefore, the early advance of the interface up to the point of precipitate nucleation, point N in Figure 9, must occur by repetitive formation of ledges and their sideways motion. As the incoherent superledges move to the right and left in the figure, they will enter material with an initial matrix content of V. The V will be transported downward in the interface to the growing V(C,N) particles in the lower row by fast boundary diffusion. This creates a V gradient in the superledge to be inherited by the ferrite, yielding a profile shown schematically in the figure.

It is reasonable to assume that boundary diffusion will be much smaller in the semicoherent  $\{111\}_\gamma/\{110\}_\alpha$  interface as compared to diffusion in the incoherent superledge. This

justifies that V diffusion from the moving superledge back to V(C,N) particles formed in the semicoherent front interface is neglected and that the formation of V(C,N) in the new precipitate sheet lags somewhat behind the moving superledge. Furthermore, as discussed in the preceding section, volume diffusion can be neglected. It is reasonable to assume that the semicoherent  $\gamma/\alpha$  interface bends over rather sharply into the superledge and not smoothly, because of the low energy of the semicoherent part of the interface (Figure 9).

Neglecting the diffusion in the semicoherent  $\gamma/\alpha$  facet and all volume diffusion, the problem consisting of the diffusional flow of V to V(C,N) particles at the lower end of the superledge, as the ledge moves into material with an initial V content, has been solved analytically.<sup>[25,26]</sup> The V gradient in the section A–B in Figure 9, just behind the moving ledge, is predicted to be

$$\frac{c_V^0 - c_V^{\alpha/\gamma}}{c_V^{\alpha/\gamma} - c_V^{\alpha/\text{VCN}}} = \frac{\cosh(x\sqrt{a/2\lambda})}{\cosh(\sqrt{a/2})} \quad [7]$$

where the meaning of the symbols  $c_V^{\alpha/\gamma}$ ,  $c_V^0$ ,  $c_V^{\alpha/\text{VCN}}$ ,  $x$ , and  $\lambda$  are given in Figure 9, and

$$a = \frac{4\nu\lambda^2}{(D\delta)^{\text{boundary}}} \quad [8]$$

where  $\nu$  is the velocity of the  $\gamma/\alpha$ -interface superledge and  $(D\delta)^{\text{boundary}}$  is the diffusion coefficient in the interface. The parameter  $x$  should actually be measured along the superledge, which is curved, according to the upper part of Figure 9. That curvature is neglected where the abscissa is denoted by  $x$  in the lower part of the figure. At  $x = 0$ , this expression generates the V content of ferrite in the upper end of the superledge, and when this reaches the critical value for V(C,N) nucleation, we get the condition for the intersheet spacing.

$$\frac{c_V^0 - c_V^{\alpha/\gamma^*}}{c_V^0 - c_V^{\alpha/\text{VCN}}} = \frac{1}{\cosh\sqrt{a/2}} \quad [9]$$

As one could anticipate, Eq. [7] predicts that the V content of ferrite in the  $\gamma/\alpha$  interface increases gradually as the interface bulge advances from the gap in the lower-particle row. When the foremost part of the bulge has reached the V content necessary for V(C,N) nucleation, a new row is initiated and will gradually grow laterally as the superledge advances.

A consequence of interphase precipitation in semicoherent  $\gamma/\alpha$  interfaces may be that there is only limited growth of the precipitates in the foremost row after nucleation, due to the slow boundary diffusion in these boundaries. Most of their growth may occur in a second stage when the interface has bulged out and a superledge moves along the row of particles. This is indicated by different precipitate sizes in Figure 9.

For computations of the V content of ferrite in the  $\gamma/\alpha$  interface and of the intersheet spacing ( $\lambda$ ), we need to know the velocity of the superledge. The lateral motion of the ledge along the intersheet requires transfer of C from the newly formed ferrite into the austenite. Since the superledge moves along the  $\gamma/\alpha$  interface, which has already received C by the formation of  $\alpha$ , it may be assumed that the advance of the superledge will be controlled by lateral transfer of C and its diffusion in the gradient normal to the precipitate

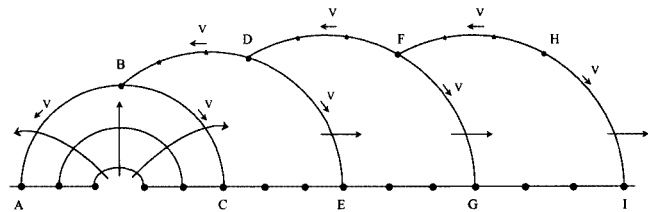


Fig. 10—Schematic drawing showing interphase precipitation in an incoherent  $\gamma/\alpha$  interface. See text for explanation. The filled circles in the front designate the primary precipitates first formed, and the particles drawn as stars are formed somewhat later in the stationary, shallow bows.

sheet. Under these conditions, we suggest that the expression for planar growth of ferrite (Eqs. [3] and [4]) gives a reasonable description also of the growth of the superledge.

The present account of interphase precipitation is obviously restricted to cases where the boundary diffusion in the  $\gamma/\alpha$  interface parallel to the precipitate sheet is very low, as in the  $\{111\}_\gamma/\{110\}_\alpha$  facets discussed previously. It is, however, well demonstrated that interphase precipitation with regular intersheet spacings may also occur in incoherent, often-curved  $\gamma/\alpha$  boundaries.<sup>[11]</sup> The principal difference between this case and the case of semicoherent interfaces discussed previously arises when the bulge has bowed out sufficiently for a new precipitate sheet to be nucleated (point N in Figure 9). In the case of a semicoherent interface, the diffusional flow of V will occur in one direction of the superledge, from the foremost part of the ledge to the precipitates in the previous sheet, whereas the flow can take place both to the new particle in the front row and to the particles in the preceding row when all of the  $\gamma/\alpha$  interface is incoherent.

The drawing in Figure 10 attempts to describe how we believe that interphase precipitation with distinct rows of particles in periodic spacings develops under these conditions. The events up to the first-formed precipitate in the new row, B in Figure 10, are similar to the case of semicoherent  $\gamma/\alpha$  interfaces. As previously (Figure 9), we assume that the  $\gamma/\alpha$  interface, pinned by the particles in the lower row, breaks away when the interface cusp at the particle has reached a critical angle. We will rather arbitrarily choose it to be 90 deg, but realize that it should be somewhat higher. Figure 10 shows how the right-hand part of the original bulge (BC) moves to the right by ferrite growth and successive unpinning of the interface from the particles in the lower row. As the ferrite grows, V diffusion in the migrating interface will occur both to the foremost particle (B) and to the particles in the lower row. This will create a solute-concentration profile in the interface, to be inherited by the ferrite, with a maximum approximately in the middle of the bow. As the bow grows, this maximum V content increases, and, when it reaches the critical value for nucleation, a new precipitate forms. The lower part of the bow repeats the process described. In this way, a series of primary precipitates will form in the front row. The shallow bows facing upward in Figure 10 will rapidly become permanently arrested after the formation of the primary precipitates. The arrest is due to dense precipitation that makes bulging between particles impossible for particle spacings below  $\sim 50$  nm at 750 °C (*cf.*, Section II), an effect which soon will be strengthened by further precipitation in the interface segments BD, DF, and FH (Figure 9). In addition, the large

interface cusp angles make breakaway at the particles impossible. Hence, in this way, we can expect a dense precipitation in the sheet to form in much the same way as in the case of semicoherent interfaces (Figure 9). The waviness of the interphase precipitation, as indicated in Figure 10, is likely to be smoothed during the formation of the next precipitate sheet, due to particle growth affected by the surface-tension forces of the corrugated sheet.

The construction of the new row of precipitation in Figure 10 is based on the assumption that the sites for nucleation of the primary precipitates will be defined by equal diffusion distances from the points of maximum V content at the centers of the circular bows (B, D, F, and H) to their end points (A–C, B–E, D–G, and F–I, respectively). This, together with the breakaway angle of 90 deg of the interface cusps along C–I, defines the geometry of the construction. The mathematical treatment of the diffusional flow in the  $\alpha/\gamma$  interface is more complex than in the previous case leading to Eq. [7], because of the varying interface velocity over the swinging bow (BDE, DFG, *etc.* in Figure 10). However, we suggest that the assumption of a maximum V content at the centers of the bows is reasonable. Furthermore, we expect that the diffusion distances (BC, DE, FG, *etc.*) creating the condition for precipitate nucleation should be approximately the same as in the case of semicoherent interfaces (AB in Figure 9).\*

\*A consequence of the geometric construction for the lateral motion of the  $\alpha/\gamma$  interface bows (BC, DE, *etc.* in Figure 10) is that the interface velocity varies along the bow length, linearly growing from a zero value at the pivot points (B, D, *etc.*) and to a maximum at the end of the bows (C, E, *etc.*). The diffusion equation describing the redistribution of solutes in the interface becomes more complex than in the case with a constant interface velocity, resulting in Eq. [7]. However, there is also an analytical solution in this case involving the so-called Airy wave functions.<sup>[27]</sup> The solution for the present boundary conditions has been analyzed for the 0.10C-0.12V-0.010N steel aged at 750 °C,<sup>[28]</sup> and the main results are as follows. The maximum V content in the interface is slightly shifted to the previous precipitate sheet; the length of DE is 42 pct of that of BDE. The bow length needed to reach the critical V content for nucleation is 38 pct larger than the length of the original bow (ABC), which expands at a constant rate along the bow. Hence, BDE, DFG, *etc.* are 1.38 times longer than ABC. The circular bows converge rapidly to a constant size, as noted previously, and this results in a convergence in row spacing at 1.57 times the radius of the original bow (ABC). Since the bow length BC is  $\pi/2$ , or 1.57 times the radius of ABC, and this length corresponds to the diffusion distance and the row spacing for the case of semicoherent interfaces, this leads to a perfect match between the spacings for the two cases considered.

What also needs to be proven is that the intersheet spacing soon converges to a fixed value. For the conditions used in Figure 10, it is readily shown that this is so. From the figure, we can see that the spacing from the original bulge to the second increases by about 25 pct. But from the third bow, it has already converged to a stable value of 1.30 times the spacing of the original bow. By comparing the geometry of interphase precipitation according to Figure 9 with that of Figure 10, it is found that, for the same diffusion distance in the super ledge, the intersheet spacings for the cases of incoherent and semicoherent  $\gamma/\alpha$  interfaces will differ by less than 20 pct. On the basis of this, we therefore suggest that the quantitative model presented in Eqs. [7] through [9] will be a reasonable approximation also for interphase precipitation in incoherent  $\gamma/\alpha$  interfaces.

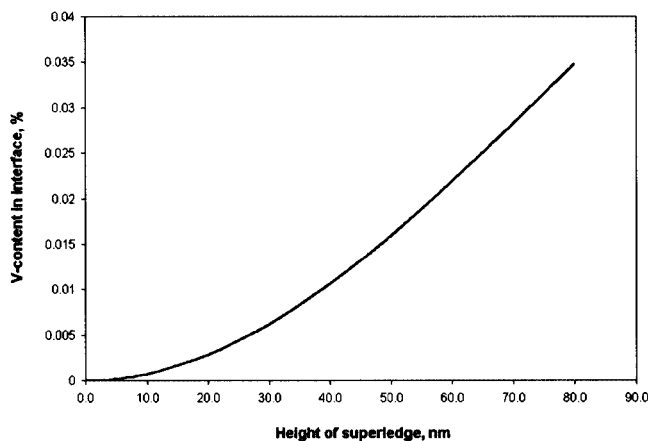


Fig. 11—Variation of V content of ferrite in the  $\gamma/\alpha$  interface with the height of the superledge according to the boundary diffusion model.

## VI. PREDICTIONS OF THE MODEL BASED ON BOUNDARY DIFFUSION AND COMPARISON WITH EXPERIMENTAL RESULTS

By employing data for the equilibrium concentrations in Eqs. [3], [4], [8], and [9] from the special microalloy database within Thermo-Calc<sup>[20]</sup> and for other parameters from the literature, the intersheet spacing can be computed, and predictions of its dependence on various interesting parameters such as the temperature and the carbon, vanadium, and nitrogen contents of the steel can be made. The velocity of the  $\gamma/\alpha$  interface varies inversely with the distance of ferrite growth ( $S$ ), Eq. [4], and, therefore, the predicted intersheet spacing will also depend on this distance (Eq. [8]). The significance of this will be discussed later. For the computations made subsequently, the assumption will be made that the ferrite has grown to a fixed size of 5  $\mu\text{m}$ . For a final grain size of 10  $\mu\text{m}$ , this means that the  $\gamma/\alpha$  transformation has proceeded to 50 pct.

We have found no data for diffusion of V in  $\gamma/\alpha$  interfaces or grain boundaries of  $\gamma$  or  $\alpha$ . We have, therefore, chosen to fit the computed intersheet spacing to the experimental value at one point, *viz.*, the spacing for a 0.10C-0.12V-0.010N steel isothermally held at 750 °C, and to use the diffusion coefficient as the adjusting parameter. This generates a diffusion coefficient  $((D\delta)^{\text{boundary}})$  of  $5.3 \cdot 10^{-12} \text{ mm}^2/\text{s}$  at 750 °C. If we compare this with reported data for grain-boundary diffusion of iron in  $\gamma$  and  $\alpha$ ,  $(D\delta)^{\text{boundary}} = 5.4 \cdot 10^{-5} \exp(-155,000/RT)$ ,<sup>[24]</sup> the present value is 8 times larger. We consider this as good an agreement as can be expected in view of normal experimental scatter in reported diffusion data and the plausible differences between interface diffusion of V and grain-boundary diffusion of Fe. In the following computations, we will, therefore, use the reported diffusion coefficient for grain-boundary diffusion of Fe multiplied by 8.

Figure 11 shows how the V concentration of ferrite in the  $\gamma/\alpha$  interface (Figure 9) varies with the height of the superledge, according to the boundary-diffusion model. By comparing this with Figure 8, we note that this model drains V more effectively at short distances than the model based on volume diffusion.



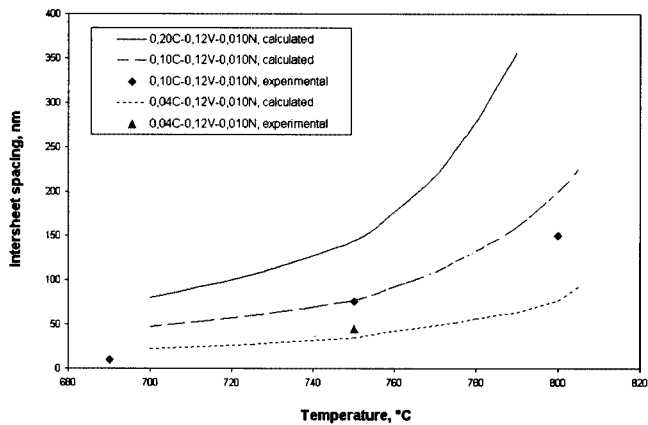


Fig. 12—Calculated variation of the intersheet spacing with temperature for 0.12V-0.010N steels at three levels of C content, 0.04, 0.10, and 0.20 wt pct. Experimental data from Ref. 2 are given for comparison.

The predicted variation of intersheet spacings with temperature for 0.12V-0.010N steels at three levels of C content (0.04, 0.10, and 0.20 wt pct) is shown in Figure 12. Experimentally measured values are also inserted.<sup>[2]</sup> The spacings become progressively smaller with decreasing temperature. The physical cause of this is that the critical V content of ferrite in the  $\gamma/\alpha$  interface for V(C,N) nucleation is reached for shorter distances, due to the fact the diffusional flow of V decreases more on lowering the temperature than does the ferrite growth.

The observed temperature dependence of the intersheet spacing is reasonably well predicted on going from 750 °C to 800 °C, whereas the relative deviation on going to 700 °C is considerably larger. It appears that this larger deviation may be related to the fact that local equilibrium in the moving interface can no longer be maintained below 700 °C, and a paraequilibrium with a uniform V content across the interface prevails. Hence, this will augment the V content of  $\gamma$  in the  $\gamma/\alpha$  interface over that of the equilibrium and will, therefore, tend to increase the driving force for V(C,N) precipitation. In turn, this would lower the critical V content for nucleation and decrease the intersheet spacing (*cf.*, Eqs. [8] and [9]). In addition, the transition from local equilibrium to paraequilibrium changes, according to Hillert and Ågren,<sup>[23]</sup> the  $\gamma/\alpha$  and the  $\alpha/\gamma$  boundaries of the phase diagram, such that the C diffusion-controlled  $\gamma/\alpha$  transformation will be driven by a larger difference in C activity. This will increase the interface velocity relative to that expected for local equilibrium. Hence, this effect will also tend to decrease the intersheet spacing, according to Eq. [8]. Thus, the inclusion of these two effects of paraequilibrium would seem to improve the agreement at 700 °C. The declining intersheet spacings with decreasing temperatures indicate that the mechanism of interphase precipitation eventually breaks down somewhere below 700 °C. According to the model, the basic cause of this transition is that the  $\gamma/\alpha$  interface velocity becomes too fast, compared to the V diffusion, for nucleation and growth of V(C,N) to take place in the moving interface. This will leave ferrite supersaturated with respect to V(C,N) and produce a general precipitation in ferrite after the passage of the  $\gamma/\alpha$  interface.

As the temperature is raised, we should notice that both

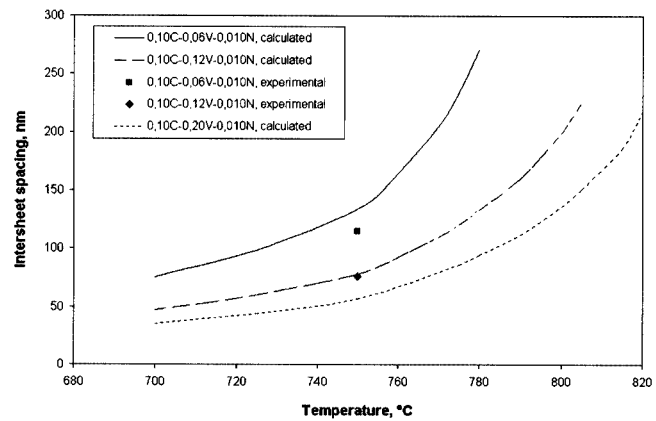


Fig. 13—Calculated variation of the intersheet spacing with temperature for 0.10C-0.010N steels at three levels of V content: 0.06, 0.12, and 0.20 wt pct. Experimental data<sup>[2]</sup> are given for comparison.

the critical V content for interphase nucleation, and the solubility of V(C,N) in ferrite increase, but  $c_V^{\alpha/\gamma^*}$  will always be larger than  $c_V^{\alpha/\gamma}$ . In the relationship between these V contents and the intersheet spacing (Eq. [9]), this implies that, at a critical temperature,  $c_V^{\alpha/\gamma^*}$  approaches the V content of the matrix,  $c_V^0$ ; hence, the left-hand side of Eq. [9] goes to zero. In turn, this means that  $\lambda$  approaches infinity asymptotically. Physically-chemically, this is, of course, expected, since at this critical temperature the V content is nowhere near high enough for nucleation to occur in moving  $\alpha/\gamma$  boundaries. For the 0.12 and 0.20 pct V steels, the critical temperatures are far above the range of data deduced in Table I. For the 0.06 pct V steel, the data of Table I give a critical temperature of 801 °C.

As demonstrated in Figure 12, the model predicts that the intersheet spacing increases with the C content of the steel. This is a result of the reduced growth rate of ferrite with increasing C content. At 750 °C, we have measured spacings at two C levels (0.10 to 0.04 pct), and the predicted decrease of the spacing on lowering the C content is in close accord with the observation.

Figure 13 shows in a similar fashion the temperature dependence for three different V contents in 0.10C-0.010N steels. The model predicts that the intersheet spacing increases as the V level is lowered. Physically, this can be considered to be a result of the fact that, at low V levels, the interface must advance further to build up the necessary V content for V(C,N) nucleation in the interface. The predicted increase of the spacing by decreasing the V content from 0.12 to 0.06 pct agrees, again, quite well with observed values (Figure 13).

Figure 14 displays a comparison between the computed and observed intersheet spacings in 0.10C-0.12V steels with N contents varying from 0.005 to 0.020 pct. The spacing declines rather strongly with higher N contents. The physical-chemical explanation of this is that the necessary chemical driving force for V(C,N) nucleation in the  $\gamma/\alpha$  interface is reached for a lower V content as the N content is increased. According to Eqs. [8] and [9], this generates smaller spacings. The matching between computed and experimental data is quite striking (Figure 14).

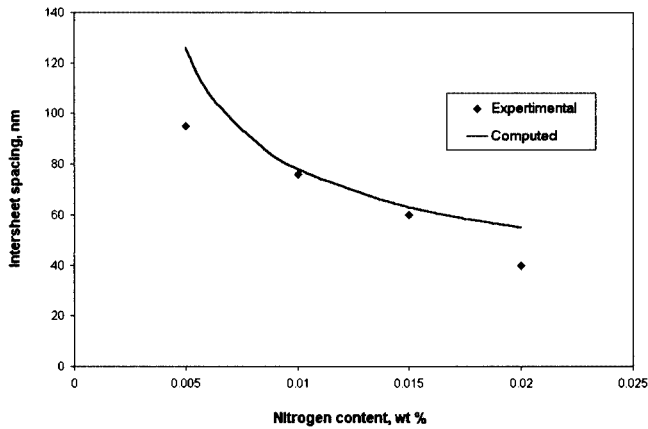


Fig. 14—Comparison between computed and observed intersheet spacings<sup>[2]</sup> in 0.10C-0.12V steels aged at 750 °C as a function of N content.

A corollary of the present model for interphase precipitation is that the  $\gamma/\alpha$  interface is stationary over nearly all its length, due to precipitate pinning. Its motion occurs only by the lateral motion of the superledges. From this, it follows that the average overall interface velocity ( $\nu^{\text{total}}$ ) will be given by the ledge velocity reduced by a factor of  $\lambda/b$ , where  $\lambda$  is the intersheet spacing and  $b$  is the average ledge spacing along the precipitate sheet,

$$\nu^{\text{total}} = \nu\lambda/b \quad [10]$$

This presents a simple and natural explanation for why vanadium slows down the  $\gamma/\alpha$  transformation.<sup>[29]</sup>

By combining Eqs. [4] and [8], we find that the model predicts the intersheet spacing to increase with the square root of the distance of ferrite growth, according to the following expression:

$$\lambda = \left( \frac{a(D\delta)^{\text{boundary}} S}{2K_1} \right)^{1/2} \quad [11]$$

From the reasoning leading to Eq. [10], it follows that the average dwell time of the  $\gamma/\alpha$  interface at each precipitate row is the superledge spacing divided by the ledge velocity ( $b/\nu$ ). Since  $\nu$  increases with a declining  $S$  value, this implies that there will be progressively less time for V(C,N) nucleation in the early stages of this stepwise ferrite growth.

Hence, on lowering  $S$ , the precipitate density will become gradually more sparse, and eventually it will virtually vanish. We may state that an interphase precipitation with a particle spacing within the precipitate sheet of the same size as the intersheet spacing can definitely not be distinguished in the electron microscope. More realistically, the former should perhaps be about one-third of the size of the latter for identification to be possible. Quantitatively, the interrelations between the intersheet spacing, the precipitate spacing in the precipitate sheet ( $\Lambda$ ), and  $S$  can be obtained in the following way. By means of the  $\gamma/\alpha$ -interface velocity (Eq. [4]), the effective interface width ( $w$ ), and the classical expression for the nucleation rate (Eq. [1]), we can express the number of nuclei formed during the time interval when the interphase precipitation is being formed.

$$n = Jwb/\nu \quad [12]$$

For the sake of simplicity, we will assume  $b$  to be constant.

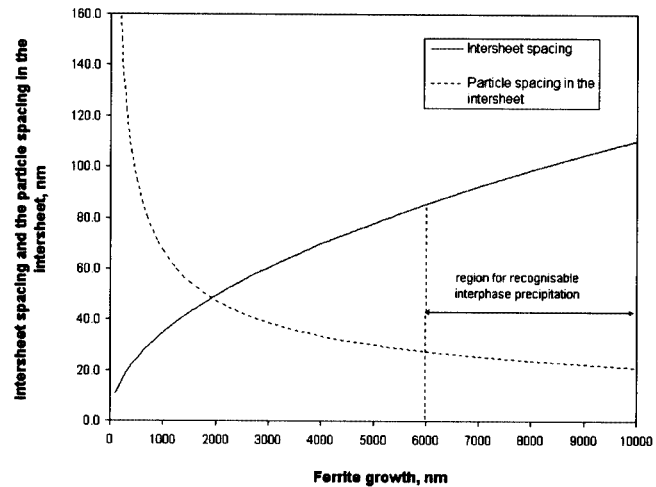


Fig. 15—Variation of intersheet spacing and particle spacing within a precipitate sheet in a ferrite grain with a size of 10  $\mu\text{m}$  and a demonstration of the area where interphase precipitation is recognizable.

The precipitate spacing in the sheet is approximately equal to  $1/(n)^{1/2}$ , and combining this with Eq. [4] gives the following relationship between  $\Lambda$  and  $S$ :

$$\Lambda = A/(S)^{1/2} \quad [13]$$

where  $A$  is a constant for a given steel and aging condition. By applying the expressions for  $\lambda$ , (Eq. [11]) and  $\Lambda$  (Eq. [13]) to the observed values for the 0.10C-0.12V-0.0082N steel (Figure 1) and assuming that the observations have been made at  $S = 5000$  nm, we can calculate the variation of intersheet spacing and particle spacing in the sheet with the distance of ferrite growth (Figure 15). If we make the reasonable assumption that interphase precipitation will not be recognizable unless  $\lambda \geq 3\Lambda$  (Figure 15), interphase precipitation will only be observed for  $S$  values larger than about 6000 nm.

For a ferrite grain size of 10  $\mu\text{m}$ , this implies that we should expect a variation for  $\lambda$  from about 85 to 110 nm, or approximately 30 pct. Such a minor variation over a large distance relative to the size of the spacing is difficult to measure. It is, therefore, no surprise that such interior variations in spacings have not been observed.

Hence, we must conclude that interphase precipitation can, for the cases studied here, only be observed after a fairly substantial ferrite growth. In the very early stages, we cannot expect any V(C,N) nucleation to occur due to the high ferrite growth rate. Somewhat later, interface nucleation may occur, but will be too sparse to be identified as interphase precipitation. In this context, reference must be made to the work by Smith Dunne,<sup>[5]</sup> mentioned in Section I. They specifically noticed that interphase and general V(C,N) precipitation formed jointly in the same grain. The explanation they offered is that the first-formed ferrite may grow too rapidly for interphase precipitation to occur, subsequently leaving the ferrite supersaturated for general precipitation. Hence, this is a conclusion that is in exact agreement with the predictions of the present model.

## VII. SUMMARY AND CONCLUSIONS

1. A model for interphase precipitation in V-microalloyed steels has been developed. It is based on an analysis of

the diffusional drainage of V in the wake of a moving  $\alpha/\gamma$  boundary to a sheet of interface precipitation. The V concentration in the interface increases gradually as it advances and eventually reaches a critical value when a new row of precipitation can be nucleated. A particular aim of the model, besides being consistent with general microscopic observations of the phenomenon, has been to explain experimentally found dependencies of interphase precipitation on temperature and steel composition.

2. The condition of nucleation is evaluated as a critical V content from an abundance of electron microscopy observations in one single composition and treatment of steel. By means of the Thermo-Calc microalloy database, this content can be transformed to a chemical driving force for nucleation and, furthermore, to nucleation conditions for other temperatures and steel compositions.
3. If these basic concepts are used to build a model on volume diffusion of V, it is clearly demonstrated that predicted intersheet spacings are much lower than those observed. In fact, it is shown that the diffusion coefficient must be raised several orders of magnitude to reach agreement. Hence, it is concluded that a mechanism must be found where the transport of V occurs by boundary diffusion in the moving  $\alpha/\gamma$  interfaces.
4. By building on the concepts of the ledge mechanism, both for semicoherent and incoherent interfaces, it is possible to find a mechanism for sufficiently fast supply of V to the growing interphase precipitation by boundary diffusion. The lateral movement of superledges along the precipitate sheet generates a V gradient, from the front  $\alpha/\gamma$  interface to the precipitate row behind, by diffusional flow in the ledge back to the particles. Through modifications, the model can be made to function for both semicoherent and incoherent  $\alpha/\gamma$  boundaries. The growth of ferrite into austenite by advancing  $\alpha/\gamma$  superledges is assumed to be controlled by lateral transfer of C and its diffusion in the gradient normal to the precipitate sheet. The model can be expressed in analytical form, resulting in rather simple expressions for the dependence of the intersheet spacing on temperature and steel composition, such as the C, V, and N content.
5. Due to lack of data for diffusion of V in  $\alpha/\gamma$  or grain boundaries, we have chosen to fit the computed intersheet spacing to that observed at *one* point by adjusting the boundary-diffusion coefficient. The coefficient so obtained was 8 times larger than the reported experimental data for grain-boundary diffusion of Fe in  $\alpha$  and  $\gamma$ . In view of the normal experimental scatter in diffusion data and plausible differences between the interface diffusion of V and grain-boundary diffusion of Fe, we consider this to be quite a good agreement.
6. With this single fitting procedure, the model is then capable of reproducing reasonably good agreement with experimentally measured intersheet spacings, their temperature dependence, and their dependence on the C, V, and N content of the steel. It is also able to predict the transition from interphase to general precipitation to be below 700 °C for the present steel compositions, in accord with observations. The model provides physically sound and satisfactory explanations of all these dependencies.
7. Due to its relation to the  $\alpha/\gamma$  velocity, the intersheet spacing is predicted to increase with the square root of

the ferrite growth. However, the rapid ferrite growth in the early stage of the  $\gamma/\alpha$  transformation results in no or only sparse nucleation of V(C,N) in the interface. Hence, this leaves the ferrite supersaturated and will subsequently generate a general precipitation of V(C,N), or it will produce a very deficient interphase precipitation that cannot be identified as such in the microscope. A consequence of this is that an identifiable interphase precipitation forms, typically in less than half of the ferrite volume. This conclusion of the model agrees with independent observations of other investigators.

## ACKNOWLEDGMENTS

The authors are indebted to Professor Mats Hillert for constructive criticism and rewarding and stimulating discussions leading to the concepts of interphase precipitation controlled by boundary diffusion in moving superledges. Thanks are also due to Professor Bevis Hutchinson for valuable discussions of the manuscript.

## REFERENCES

1. F.A. Khalid and D.V. Edmonds: *Mater. Sci. Technol.*, 1993, vol. 9, pp. 384-96.
2. S. Zajac, T. Siwecki, and M. Korchynsky: *Proc. Int. Symp. Low Carbon Steels for the 90's*, ASM/TMS Materials Week, Pittsburgh, PA, Oct. 17-21, 1993, pp. 139-50.
3. S. Zajac, R. Lagneborg, and T. Siwecki: *Proc. Int. Conf. Microalloying '95*, ISS, Pittsburgh, PA, 1995 pp. 321-40.
4. R.G. Baker and J. Nutting: *Precipitation Processes in Steels*, ISI Report No. 64, ISI, London, 1969 pp. 1-22.
5. R.M. Smith and D.P. Dunne: *Mater. Forum*, 1988, vol. 11, pp. 166-81.
6. R.W.K. Honeycombe: *Proc. Int. Conf. on Technology and Applications of HSLA Steels*, ASM, Metals Park, OH, 1983, pp. 243-50.
7. W.C. Johnson, C.L. White, P.E. Marth, P.R. Ruf, S.M. Tuominen, K.D. Wade, K.C. Russell, and H.I. Aaronson: *Metall. Trans. A*, 1975, vol. 6A, pp. 911-19.
8. J.L. Lee and H.I. Aaronson: *Acta Metall.*, 1975, vol. 23, pp. 799-808.
9. A.T. Davenport and R.W.K. Honeycombe: *Proc. R. Soc. London*, 1971, vol. 322, pp. 191-205.
10. R.W.K. Honeycombe: *Metall. Trans. A*, 1976, vol. 7A, pp. 915-36.
11. R.A. Ricks and P.R. Howell: *Acta Metall.*, 1983, vol. 31, pp. 853-61.
12. W. Roberts: Internal Report IM-1333, Swedish Institute for Metals Research, Stockholm, 1978.
13. A.D. Batte and R.W.K. Honeycombe: *J. Iron Steel Inst.*, 1973, vol. 211, pp. 284-89.
14. M. Hillert: *Phase Diagrams and Phase Transformations*, Cambridge University Press, Cambridge, MA, 1998.
15. G.R. Purdy and J.S. Kirkaldy: *Trans. TMS-AIME*, 1963, vol. 227, pp. 1255-56.
16. M. Hillert: *Metall. Trans. A*, 1975, vol. 6A, pp. 5-19.
17. M. Hillert and J. Ågren: *Advances in Phase Transitions*, J.D. Embury and G.R. Purdy, eds., Pergamon Press, Elmsford, NY, 1988, pp. 1-19.
18. R.A. Ricks and P.R. Howell: *Met. Sci.*, 1982, vol. 16, pp. 317-21.
19. B. Sundman, B. Jansson, and J.O. Andersson: *CALPHAD*, 1985, vol. 9, pp. 153-59.
20. S. Zajac: Report IM-3566, Swedish Institute for Metals Research, Stockholm, 1998.
21. K.C. Russell: *Adv. Colloid Interface Sci.*, 1980, vol. 13, pp. 205-318.
22. W.J. Liu, E.B. Hawbolt, and I.V. Samarasekara: *Proc. Int. Symp. on Mathematical Modelling of Hot Rolling of Steel*, S. Yue, ed., CIM, Hamilton, 1990, pp. 477-87.
23. M. Hillert and J. Ågren: *Diffusion and Equilibria—an Advanced Course in Physical Metallurgy*, Royal Institute of Technology, Stockholm, 1997.

24. J. Fridberg, L.-E. Törndahl, and M. Hillert: *Jernkont. Ann.*, 1969, vol. 153, pp. 263-76.
25. J.W. Cahn: *Acta Metall.*, 1959, vol. 7, pp. 18-28.
26. M. Hillert: *Proc. Int. Symp. on the Mechanism of Phase Transformation in Crystalline Solids*, Monograph and Report Series No. 33, Institute of Metals, London, 1969, pp. 231-49.
27. Computer software, MATLAB, MathWorks Co., 1999.
28. R. Lagneborg: Report IM-2000-012, Swedish Institute for Metals Research, Stockholm, 2000.
29. F.B. Pickering: *Proc. Int. Conf. on High Nitrogen Steels—Technology and Applications*, HNS 88, J. Vogt and A. Henry, eds., The Institute of Metals, London, 1989, pp. 10-31.